Dyes and Pigments 95 (2012) 512–522

Contents lists available at SciVerse ScienceDirect

Dyes and Pigments

journal homepage: www.elsevier.com/locate/dyepig

The synthesis, structure and photoluminescent properties of solid-state green to yellow emitters based on β-carboline

Yi-Feng Sun [a,b,*], Zhi-Yong Chen [a], Ya-Ling Liu [a], Na Li [a], Ji-Kun Li [b], Hua-Can Song [a]

[a] Guangdong Provincial Public Laboratory of Analysis and Testing Technology, China National Analytical Center, Guangzhou 510070, PR China
[b] School of Chemistry and Chemical Engineering, Taishan University, Taian 271021, PR China

ARTICLE INFO

Article history:
Received 10 May 2012
Received in revised form
2 June 2012
Accepted 5 June 2012
Available online 12 June 2012

Keywords:
β-Carboline
Acylhydrazone
Synthesis
Crystal structure
Emission enhancement
Photoluminescence

ABSTRACT

A series of solid-state green to yellow emitters based on β-carboline core were synthesized and characterized. The crystal structures of four of them were determined by single crystal X-ray diffraction analysis. The photoluminescent properties of β-carbolines were examined in solution and in the solid state. It was found that these fluorophores were luminescent, having solid-state emission at wavelengths ranging from 505 to 582 nm, depending on structure. Significantly, two naphthalene-carboline hybrids exhibit strong green fluorescence emission both in solution and in crystalline state. However, two methoxyl-phenyl substituted β-carboline derivative show intense green/yellow emission peaked at 540–582 nm, and display red-shifted by 40–82 nm with respect to the solution behavior. The experimental results demonstrated that the solid-state emission ranging from green to yellow can be readily tuned by simply varying molecular structure. The solid-state luminescent properties are highly dependent on the nature and position of the substituents and also on the molecular arrangements and the intermolecular interactions.

1. Introduction

The β-carboline unit, a tricyclic nitrogen-containing pharmacophore constituted by the fusion of an indole ring and a pyridine ring, can be found in a great many bioactive compounds of both natural and synthetic origin. β-Carboline derivatives have long been recognized to possess an extremely wide span of interesting biological activities [1–3], especially the central nervous system (CNS) and antitumor properties. Therefore, great efforts have been devoted to the synthesis and biological evaluation of various new β-carboline alkaloids [4–10]. Furthermore, studies on structure–activity relationship have demonstrated the influence of the position and nature of ring-substituents on the activity of β-carboline derivatives. For example, the introduction of appropriated substituents into position-1, -2, -3 and -9 of the β-carboline skeleton resulted in more potent antitumor derivatives, with decreasing acute toxicity [11,12]. Moreover, previous research has suggested that substitution at the position-3 of a β-carboline with an ester function was necessary for the high affinity binding to the central benzodiazepine receptors (BZR), and the BZR recognized preferentially the *s-cis* conformation of 3-carboxy-β-carbolines or one approaching this geometry [13].

Apart from their pharmacological properties, this class of compounds is good fluorophores [14], and has also been used as photosensitizers with potential application in photodynamic therapy [15], and as fluorescent standards [16–18] or as indicators for small acidities in the physiological pH range [14]. Besides, β-carbolines have also been reported to be capable of experiencing phototautomerism [19].

In fact, much recent attention has been focused mainly on the synthesis, characterization and biological evaluation of β-carboline derivatives, whereas less explored are their structure and photophysical properties, although some cases have been described in the literature [20–24]. In particular, only a few simple β-carbolines are employed in these studies, such as norharman, harman, harmine and methyl β-carboline-3-carboxylate (βCCM) (Fig. 1). To the best of our knowledge, however, unlike the carbazole analogs, β-carbolines have never been investigated previously for their solid-state luminescent properties.

In view of the emission properties and potential applications of these compounds, and the continued interest in the development of solid-state organic luminescent materials, the focus of the current research workers turned toward the synthesis, crystallography and optical evaluation of novel β-carboline derivatives. The solid-state photoluminescent properties of novel β-carbolines are

* Corresponding author. School of Chemistry and Chemical Engineering, Taishan University, Taian 271021, PR China. Tel.: +86 20 37656300; fax: +86 20 87686511.
E-mail address: sunyf50@yahoo.com.cn (Y.-F. Sun).

0143-7208/$ – see front matter © 2012 Elsevier Ltd. All rights reserved.
http://dx.doi.org/10.1016/j.dyepig.2012.06.002

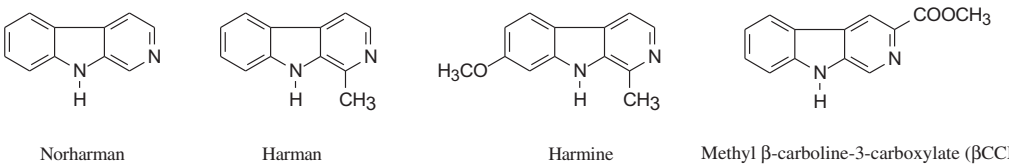

Fig. 1. The structures of Norharman, Harman, Harmine and βCCM.

discussed. The structures were investigated to obtain insights on the possible origins of solid-state luminescent properties. The synthetic pathway and the structures of target molecules are shown in Figs. 2 and 3.

2. Experimental

2.1. General

^{1}H NMR and ^{13}C NMR spectra were taken on a Bruker AVANCE-300 NMR spectrometer and chemical shifts expressed as δ (ppm) values with TMS as internal standard. Element analysis was taken with a Perkin–Elmer 240 analyzer. Mass spectra (MS) were measured on an Agilent LC/MSD Trap XCT mass spectrometer with an electrospray ionization source in positive ion mode. Absorption spectra were determined on a Hitachi U-3900 UV–Vis scanning spectrophotometer. The solution phase photoluminescence spectra were determined with a Hitachi F-2500 spectrometer and the slit widths were 5 nm for both excitation and emission. The solid-state photoluminescence spectra were measured using a Horiba Jobin-Yvon LabRam HR UV-NIR Confocal Laser MicroRaman spectrometer under a 325 nm He–Cd laser excitation. Single crystal was characterized by Bruker Smart 1000 CCD X-ray single-crystal diffractometer. The melting points were determined with a WRS-1A melting point apparatus and are uncorrected. All reagents and chemicals are commercially available and used without further purification. The starting compounds **2** were prepared according to reported methods [11,25,26].

2.2. Synthesis of β-carboline-3-carbohydrazides (**3**)

2.2.1. β-Carboline-3-carbohydrazide (**3a**)

80% hydrazine hydrate (20 mL) was added to the suspension of **2a** (8 mmol) in ethanol (80 mL), the mixture was refluxed for 7 h. After cooling, the precipitate was collected by filtration, washed with ethanol, and then dried. The crude product was recrystallized from ethanol to give **3a** as silver plates, yield 71%, mp > 250 °C (Lit. mp 289–291 °C [27]).

2.2.2. 9-Benzyl-β-carboline-3-carbohydrazide (**3b**)

This compound was prepared from **2b** and hydrazine hydrate according to the procedure described for **3a**. Colorless crystals, yield 68%; mp 207–209 °C (Lit. 209–211 °C [28]) ; ^{1}H NMR (300 MHz, DMSO-d_6/TMS) δ: 4.59 (s, 2H), 5.86 (s, 2H), 7.22–7.32 (m, 5H), 7.35 (t, J = 7.8 Hz, 1H), 7.65 (t, J = 8.1 Hz, 1H), 7.81 (d, J = 8.4 Hz, 1H), 8.47 (d, J = 7.8 Hz, 1H), 8.87 (d, J = 0.6 Hz, 1H), 9.08 (d, J = 0.6 Hz, 1H), 9.74 (s, 1H). ^{13}C NMR (75 MHz, DMSO-d_6/TMS) δ: 46.08, 110.74, 113.75, 120.40, 120.86, 122.49, 126.84, 127.53, 128.02, 128.69, 128.87, 131.45, 137.17, 139.92, 141.27, 163.80. Anal. calcd for $C_{19}H_{16}N_4O$: C 72.14, H 5.10, N 17.71; found: C 72.21, H 5.19, N 17.62.

2.3. Synthesis of N′-arylidene-β-carboline-3-carbohydrazides (**4**)

A mixture of β-carboline-3-carbohydrazides **3** (2 mmol) and the appropriate aryl aldehydes (2 mmol) in anhydrous ethanol (30 mL) was heated under reflux for 6 h. After cooling, the solid was filtrated and recrystallized from ethanol– *N*,*N*′-dimethylformamide (DMF) to afford the pure product.

2.3.1. N′-(2-hydroxyl-1-naphthylmethylene) -β-carboline-3-carbohydrazide (**4a**)

Yellow crystals, yield 69%; mp > 250 °C ; ^{1}H NMR (300 MHz, DMSO-d_6/TMS) δ: 7.26 (d, J = 9.0 Hz, 1H), 7.34 (t, J = 7.8 Hz, 1H), 7.42 (t, J = 7.2 Hz, 1H), 7.61 (d, J = 6.9 Hz, 1H), 7.66 (d, J = 8.1 Hz, 1H), 7.71 (d, J = 8.1 Hz, 1H), 7.93 (t, J = 9.3 Hz, 2H), 8.23 (d, J = 8.4 Hz, 1H), 8.47 (d, J = 7.8 Hz, 1H), 9.02 (d, J = 0.9 Hz, 1H), 9.03 (s, 1H), 9.87 (s, 1H), 12.09 (s, 1H), 12.56 (s, 1H), 13.16 (s, 1H). ^{13}C NMR (75 MHz, DMSO-d_6/TMS) δ: 108.65, 112.36, 115.26, 118.97, 120.21, 120.47, 120.88, 122.39, 123.48, 127.63, 127.75, 128.26, 128.82, 128.92, 131.81, 132.50, 137.26, 141.03, 157.96, 160.90. ESI-MS m/z: 381.4 $(M + H)^+$. Anal. calcd for $C_{23}H_{16}N_4O_2$: C 72.62, H 4.24, N 14.73; found: C 72.54, H 4.29, N 14.65.

2.3.2. N′-(2,4-dihydroxybenzlidene) -β-carboline-3-carbohydrazide (**4b**)

Off-white solid, yield 58%; mp > 250 °C ; ^{1}H NMR (300 MHz, DMSO-d_6/TMS) δ: 6.34 (d, J = 2.1 Hz, 1H), 6.38 (dd, J = 8.1, 2.1 Hz, 1H), 7.23 (d, J = 8.4 Hz, 1H), 7.31 (t, J = 8.1 Hz, 1H), 7.61 (t, J = 8.1 Hz, 1H), 7.69 (d, J = 8.4 Hz, 1H), 8.44 (d, J = 8.1 Hz, 1H), 8.73 (s, 1H), 8.96 (s, 2H), 9.99 (s, 1H), 11.82 (s, 1H), 12.04 (s, 1H), 12.27 (s, 1H). ^{13}C NMR (75 MHz, DMSO-d_6/TMS) δ: 102.70, 107.60, 110.62, 112.31, 115.01, 120.13, 120.87, 122.34, 128.21, 128.75, 131.62, 132.38, 137.34, 138.61, 141.00, 149.83, 159.61, 160.54, 160.86. ESI-MS m/z: 347.3 $(M + H)^+$. Anal. calcd for $C_{19}H_{14}N_4O_3$: C 65.89, H 4.07, N 16.18; found: C 65.81, H 4.02, N 13.91.

2.3.3. N′-(2-hydroxy-3-methoxybenzlidene) -β-carboline-3-carbohydrazide (**4c**)

Pale yellow solid, yield 60%; mp > 250 °C ; ^{1}H NMR (300 MHz, DMSO-d_6/TMS) δ: 3.85 (s, 3H), 6.90 (t, J = 7.8 Hz, 1H), 7.07 (t, J = 8.8 Hz, 2H), 7.34 (t, J = 7.5 Hz, 1H), 7.64–7.73 (m, 2H), 8.47 (d, J = 7.8 Hz, 1H), 8.88 (s, 1H), 9.00 (s, 1H), 9.02 (s, 1H), 11.49 (s, 1H),

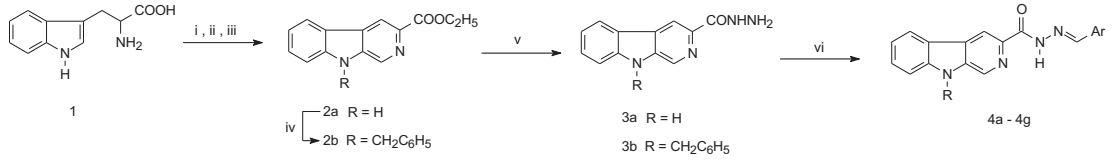

Fig. 2. Synthesis of the β-carboline-based fluorophores. Reagents and reaction conditions: (i) HCHO, NaOH; (ii) EtOH, HCl; (iii) S, Xylene, reflux; (iv) Benzyl bromide, DMF, NaH, reflux; (v) $NH_2NH_2 \cdot H_2O$, EtOH, reflux; (vi) Aryl aldehyde, EtOH, Glacial acetic acid, reflux.

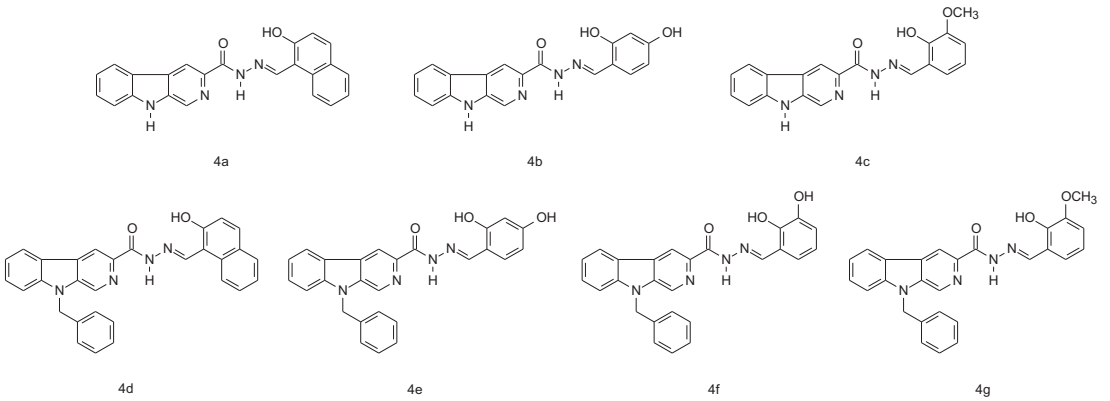

Fig. 3. The structures of the β-carboline-based fluorophores.

12.09 (s, 1H), 12.50 (s, 1H). ^{13}C NMR (75 MHz, DMSO-d_6/TMS) δ: 55.78, 112.32, 113.75, 115.25, 118.79, 118.92, 120.17, 120.87, 121.37, 122.35, 128.22, 128.78, 132.42, 137.42, 138.42, 141.01, 147.34, 147.91, 149.04, 161.21. ESI-MS *m/z*: 361.2 $(M + H)^+$. Anal. calcd for $C_{20}H_{16}N_4O_3$: C 66.66, H 4.48, N 15.55; found: C 66.52, H 4.57, N 15.63.

*2.3.4. N′-(2-hydroxyl-1-naphthylmethylene)-9-benzyl-β-carboline-3-carbohydrazide (**4d**)*

Yellow crystals, yield 66%; mp >250 °C ; ^{1}H NMR (300 MHz, DMSO-d_6/TMS) δ: 5.93 (s, 2H), 7.24–7.45 (m, 8H), 7.60–7.70 (m, 2H), 7.82 (d, J = 8.7 Hz, 1H), 7.93 (t, J = 9.4 Hz, 2H), 8.23 (d, J = 8.7 Hz, 1H), 8.53 (d, J = 7.8 Hz, 1H), 9.08 (d, J = 0.9 Hz, 1H), 9.24 (d, J = 0.9 Hz, 1H), 9.87 (s, 1H), 12.57 (s, 1H), 13.18 (s, 1H). ^{13}C NMR (75 MHz, DMSO-d_6/TMS) δ: 46.24, 108.64, 110.89, 115.14, 118.95, 120.45, 120.66, 120.86, 122.62, 123.47, 126.89, 127.60, 127.74, 128.27, 128.74, 128.91, 129.07, 131.52, 131.81, 132.49, 137.06, 137.69, 138.83, 141.36, 147.43, 157.98, 160.78. ESI-MS *m/z*: 471.5 $(M + H)^+$. Anal. calcd for $C_{30}H_{22}N_4O_2$: C 76.58, H 4.71, N 11.91; found: C 76.51, H 4.80, N 11.83.

*2.3.5. N′-(2,4-Dihydroxybenzlidene)-9-benzyl-β-carboline-3-carbohydrazide (**4e**)*

Pale yellow crystals, yield 62%; mp >250 °C ; ^{1}H NMR (300 MHz, DMSO-d_6/TMS) δ: 5.91 (s, 2H), 6.39–6.44 (m, 2H), 7.23–7.35 (m, 6H), 7.38 (t, J = 7.8 Hz, 1H), 7.65 (t, J = 8.1 Hz, 1H), 7.82 (d, J = 8.4 Hz, 1H), 8.52 (d, J = 7.8 Hz, 1H), 8.76 (s, 1H), 9.03 (d, J = 0.9 Hz, 1H), 9.20 (d, J = 0.6 Hz, 1H), 10.03 (s, 1H), 11.84 (s, 1H), 12.29 (s, 1H). ^{13}C NMR (75 MHz, DMSO-d_6/TMS) δ: 46.70, 103.22, 108.13, 111.13, 111.34, 115.42, 121.10, 121.34, 123.08, 127.36, 128.07, 128.75, 129.21, 129.53, 131.90, 132.12, 137.56, 138.05, 139.71, 141.84, 150.41, 160.14, 161.09, 161.26. ESI-MS *m/z*: 437.3 $(M + H)^+$. Anal. calcd for $C_{26}H_{20}N_4O_3$: C 71.55, H 4.62, N 12.84; found: C 71.62, H 4.71, N 12.75.

*2.3.6. N′-(2,3-Dihydroxybenzlidene)-9-benzyl-β-carboline-3-carbohydrazide (**4f**)*

Yellow crystals, yield 58%; mp 227–229 °C ; ^{1}H NMR (300 MHz, DMSO-d_6/TMS) δ: 5.92 (s, 2H), 6.78 (t, J = 7.8 Hz, 1H), 6.87–6.93 (m, 2H), 7.25–7.31 (m, 5H), 7.39 (t, J = 7.5 Hz, 1H), 7.68 (t, J = 8.4 Hz, 1H), 7.83 (d, J = 8.4 Hz, 1H), 8.53 (d, J = 7.8 Hz, 1H), 8.84 (s, 1H), 9.06 (d, J = 0.9 Hz, 1H), 9.20 (d, J = 0.6 Hz, 1H), 9.23 (s, 1H), 11.64 (s, 1H), 12.52 (s, 1H). ^{13}C NMR (75 MHz, DMSO-d_6/TMS) δ: 46.19, 110.88, 115.18, 117.29, 118.70, 119.10, 120.39, 120.66, 120.85, 122.64, 126.88, 127.59, 128.25, 128.73, 129.08, 131.48, 137.07, 137.63, 138.96, 141.35, 145.59, 146.15, 149.75, 161.10. ESI-MS *m/z*: 437.2 $(M + H)^+$. Anal. calcd for $C_{26}H_{20}N_4O_3$: C 71.55, H 4.62, N 12.84; found: C 71.59, H 4.78, N 12.67.

*2.3.7. N′-(2-hydroxy-3-methoxybenzlidene)-9-benzyl-β-carboline-3-carbohydrazide (**4g**)*

Pale yellow solid, yield 62%; mp 226–228 °C ; ^{1}H NMR (300 MHz, DMSO-d_6/TMS) δ: 3.84 (s, 3H), 5.91 (s, 2H), 6.88 (t, J = 8.1 Hz, 1H), 7.04–7.11 (m, 2H), 7.24–7.41 (m, 6H), 7.66 (t, J = 8.4 Hz, 1H), 7.83 (d, J = 8.4 Hz, 1H), 8.52 (d, J = 7.8 Hz, 1H), 8.87 (s, 1H), 9.05 (d, J = 0.9 Hz, 1H), 9.19 (d, J = 0.9 Hz, 1H), 11.44 (s, 1H), 12.47 (s, 1H). ^{13}C NMR (75 MHz, DMSO-d_6/TMS) δ: 46.21, 55.80, 110.87, 113.79, 115.15, 118.81, 118.92, 120.65, 120.86, 121.34, 122.61, 126.87, 127.58, 128.25, 128.73, 129.06, 131.45, 137.06, 137.62, 139.03, 141.36, 147.35, 147.92, 149.08, 161.10. ESI-MS *m/z*: 451.1 $(M + H)^+$. Anal. calcd for $C_{27}H_{22}N_4O_3$: C 71.99, H 4.92, N 12.44; found: C 71.87 H 4.98, N 12.35.

2.4. X-ray crystallography

X-ray quality crystals of **4b**, **4d**, **4e** and **4f** were obtained by slow evaporation of ethanol-DMF solution. The diffraction data for these four structures were collected on a Bruker Smart Apex 1000 CCD X-ray single crystal diffractometer with a graphite monochromated Mo Kα radiation (λ = 0.071,073 nm) at 298(2) K. The structures were solved by direct methods with SHELXS-97 program and refinements on F^2 were performed with SHELXL-97 program by full-matrix least-squares techniques with anisotropic thermal parameters for the non-hydrogen atoms. All H atoms were initially located in a difference Fourier map. The methyl H atoms were then constrained to an ideal geometry, with C–H = 0.096 nm and $U_{iso}(H) = 1.5U_{eq}(C)$. H atoms bonded to N and O atoms were treated as riding atoms, with N–H = 0.086 nm, O–H = 0.082–0.085 nm and $U_{iso}(H) = 1.2U_{eq}(N)$ or $U_{iso}(H) = 1.5\ U_{eq}(O)$. All of the other H atoms were placed in geometrically idealized positions and constrained to ride on their parent atoms, with C–H = 0.093–0.097 nm and $U_{iso}(H) = 1.2U_{eq}(C)$. A summary of the crystallographic data and structure refinement details is compiled in Table 1.

3. Results and discussion

3.1. Synthesis

The route used for the preparation of β-carbolines **4** was carried out as outlined in Fig. 2. Initially, the synthesis of the compounds **2** was realized in three steps starting from the commercially available L-tryptophan according to the procedure described in the literature. Subsequently, the compounds **2** were converted into β-carboline-3-carbohydrazides **3** by the treatment with 80% hydrazine hydrate in ethanol under reflux. Finally, refluxing of **3** with the properly substituted aryl aldehydes in anhydrous ethanol gave compounds **4**.

Table 1
Crystal data and structure refinement.

Compound	**4a**	**4d**	**4e**	**4f**
Empirical formula	$C_{23}H_{18}N_4O_3$	$C_{30}H_{22}N_4O_2$	$C_{55}H_{47}N_9O_7$	$C_{29}H_{27}N_5O_4$
Formula weight	398.41	470.52	946.02	509.56
Temperature (K)	298(2)	298(2)	298(2)	298(2)
Crystal system,	Orthorhombic	Monoclinic	Triclinic	Triclinic
Space group	$Pca2_1$	$P2_1/c$	$P\bar{1}$	$P\bar{1}$
Unit cell dimensions				
a (nm)	2.216(2)	0.7772(3)	1.0077(6)	1.0503(9)
b (nm)	0.6115(6)	1.8421(7)	1.0889(6)	1.1508(10)
c (nm)	1.3719(13)	1.6310(6)	2.4343(13)	1.2283(11)
α (°)	90	90	87.857(9)	64.797(14)
β (°)	90	93.822(7)	85.330(9)	81.612(13)
γ (°)	90	90	64.592(9)	76.373(14)
Volume (nm^3), Z	1.859(3), 4	2.3299(15), 4	2.405(2), 2	1.304(2), 2
D_{calc} (Mg/m^3)	1.423	1.341	1.306	1.298
Absorption coefficient (mm^{-1})	0.097	0.086	0.089	0.089
F (0 0 0)	832	984	992	536
Crystal size (mm)	0.23 × 0.12 × 0.08	0.21 × 0.16 × 0.12	0.23 × 0.18 × 0.12	0.21 × 0.16 × 0.11
θ range for data collection (°)	1.84 to 25.05	1.67 to 25.05	1.68 to 25.05	1.83 to 25.05
Limiting indices	$-26 \le h \le 25$	$-9 \le h \le 9$	$-11 \le h \le 11$	$-12 \le h \le 12$
	$-7 \le k \le 7$	$-21 \le k \le 18$	$-12 \le k \le 12$	$-13 \le k \le 9$
	$-16 \le l \le 13$	$-17 \le l \le 19$	$-28 \le l \le 20$	$-14 \le l \le 14$
Reflections collected/unique	8936/2996 [$R_{int} = 0.0842$]	11,933/4115 [$R_{int} = 0.0262$]	12,577/8412 [$R_{int} = 0.0228$]	6770/4567 [$R_{int} = 0.0148$]
Max. and min. transmission	0.9923 and 0.9780	0.9897 and 0.9821	0.9894 and 0.9799	0.9903 and 0.9816
Data/restraints/parameters	2996/0/273	4115/0/327	8412/0/645	4567/0/345
Goodness-of-fit on F^2	1.005	1.026	1.025	1.034
Final R indices	$R_1 = 0.0632$	$R_1 = 0.0390$	$R_1 = 0.0510$	$R_1 = 0.0447$
[$I > 2$sigma(I)]	$wR_2 = 0.1328$	$wR_2 = 0.0927$	$wR_2 = 0.1206$	$wR_2 = 0.1154$
R indices (all data)	$R_1 = 0.1172$	$R_1 = 0.0570$	$R_1 = 0.1030$	$R_1 = 0.0600$
	$wR_2 = 0.1609$	$wR_2 = 0.1038$	$wR_2 = 0.1502$	$wR_2 = 0.1296$
Extinction coefficient	0.0047(13)	0.0053(7)	0.0039(7)	
Largest diff. peak and hole (e.nm^{-3})	220 and 213	219 and 190	289 and 219	221 and 168
CCDC	879,674	879,675	879,676	879,677

The chemical structures of all the synthesized novel compounds were confirmed by ^{1}H NMR, ^{13}C NMR, ESI-MS and elemental analyses data. Obviously, the ^{1}H NMR spectra of all compounds **4** showed a well distinguishable intensive singlet signal at δ = 8.73–9.87 ppm for the imino proton (CH = N). Additionally, compounds **4a**–**4c** gave a characteristic singlet at δ = 12.04–12.09 ppm in DMSO, which was assigned to H-9 of the β-carboline nucleus. Nevertheless, in the cases of **4d**–**4g**, such a characteristic singlet for H-9 was absent in the ^{1}H NMR spectra, owing to the N_9-benzylation of the β-carboline nucleus.

3.2. Crystal structure

X-ray diffraction crystal structure analysis reveals that the four molecules, **4a**, **4d**, **4e** and **4f**, are remarkably similar. All four molecules adopt a *trans* configuration about the central C=N double bonds and exist in the keto–imine tautomeric form. Moreover, in each of compounds, the central hydrazone component is also effectively planar with an all-*trans* extended conformation, as exemplified by the relevant torsion angles, and the *trans* configuration of the carboxyamido carbonyl oxygen atom and the nitrogen atom of the pyridine ring can be appreciated. This is in marked contrast to the side chain conformation observed in methyl β-carboline-3-carboxylate, in which the *cis* conformation is observed [29].

Compound **4a** crystallizes in the orthorhombic space group $Pca2_1$ and has a very near planar structure with a dihedral angle of 5.2° between the naphthalene ring and the carboline ring system, which is essentially planar as expected (Fig. 4). Obviously, the N4–C13 (0.1288(6) nm) and O1–C12 (0.1224(6) nm) bonds feature C=N and C=O double bonds.

A strong intramolecular O2–H2…N4 (O2–H2…N4: O2–H2 = 0.082 nm, H2…N4 = 0.1782 nm, O2…N4 = 0.2498 nm, O2–H2…N4 = 145°) hydrogen bond is observed in the molecular structure of **4a**. Meanwhile, the molecules are linked together by intermolecular N–H…O (N1–H1…O2^{i}: N1–H1 = 0.086 nm, H1…O2 = 0.2264 nm, N1…O2 = 0.3061 nm, N1–H1…O2 = 154°, symmetry code: (i) $-x + 1, -y, z + 1/2$) hydrogen bonds into a one dimensional structure extending along the c axis (Fig. 5), which are cross-linked into a two-dimensional framework by intermolecular O–H…N, O–H…O and N–H…O hydrogen bonds (O3–H6…N2^{ii}: O3–H6 = 0.085 nm, H6…N2 = 0.2533 nm, O3…N2 = 0.3122 nm, O3–H6…N2 = 127°; O3–H7…O1: O3–H7 = 0.085 nm, H7…O1 = 0.2047 nm, O3…O1 = 0.2850 nm, O3–H7…O1 = 157°; N3–H3…O3^{iii}: N3–H3 = 0.086 nm, H3…O3 = 0.2188 nm, N3…O3 = 0.3015 nm, N3–H3…O3 = 161°;

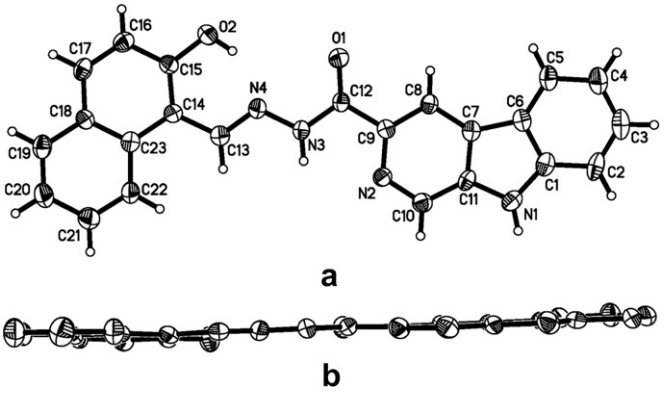

Fig. 4. (a) The molecular structure of **4a**, showing the atom-labeling scheme. Displacement ellipsoids are drawn at the 30% probability level. H atoms are shown as small spheres of arbitrary radius. Water molecule is omitted for clarity. (b) The side elevation of **4a**. Water molecule and H atoms are omitted for clarity.

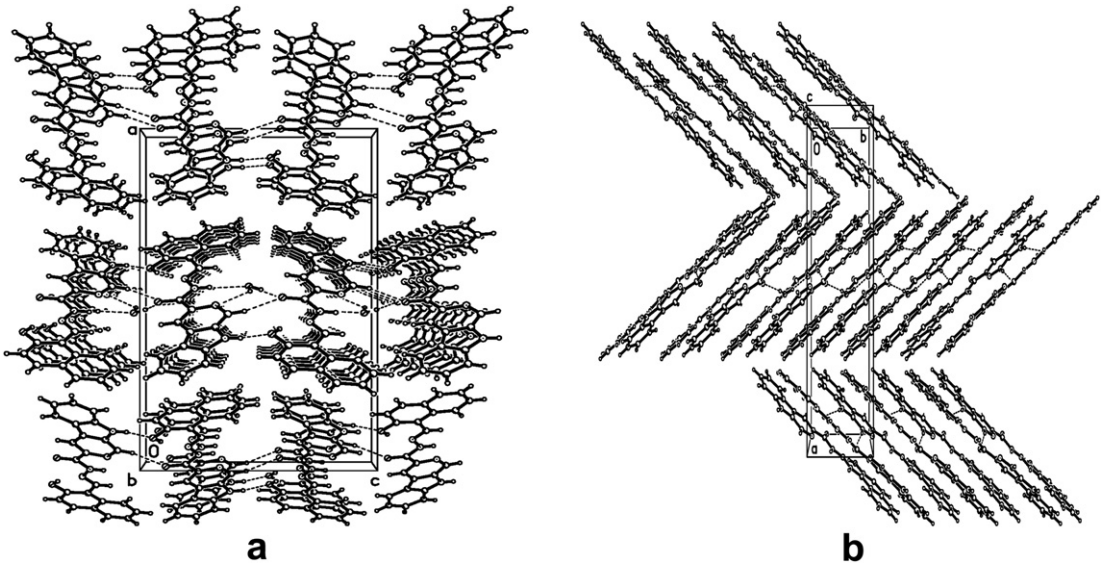

Fig. 5. Packing diagram of the cell of **4a**, viewed down the crystallographic *b* axis (a) and down the *c* axis (b).

symmetry code: (ii) $-x + 1, -y + 1, z - 1/2$; (iii) $-x + 1, -y + 1, z + 1/2$). The water molecule plays a significant role in the crystal packing as it is the acceptor in one hydrogen bond and a donor in another. As a result, the molecules are further self-assembled to form a well-ordered herringbone structure (Fig. 5).

The crystal structure of **4d** is given in Fig. 6. The compound crystallizes in monoclinic $P2_1/c$ space group. Unlike molecule **4a**, this molecule is clearly not planar due to the N_9-benzylation of the β-carboline nucleus. As can be seen from Fig. 6 , the molecule of the group carboline itself is planar, and makes a dihedral angle of 6.4° with the naphthalene ring, but forms a dihedral angle of 86.1° with the phenyl ring (Fig. 6). Thus, apart from the terminal benzyl group, the rest of the molecule lies approximately in a common

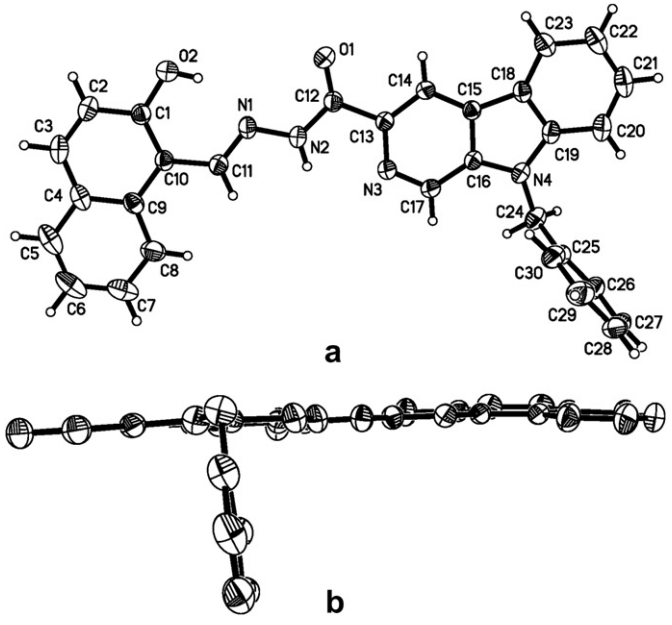

Fig. 6. (a) The molecular structure of **4d**, showing the atom-labeling scheme. Displacement ellipsoids are drawn at the 30% probability level. H atoms are shown as small spheres of arbitrary radius. (b) The side elevation of **4d**. H atoms are omitted for clarity.

plane which is almost perpendicular to the phenyl ring. Furthermore, this is evident from the observed distances of N1–C11 (0.12800(19) nm) and O1–C12 (0.12128(18) nm) which are consistent with carbon–nitrogen and carbon–oxygen double bonds, respectively.

Additionally, a stable six-membered ring can be formed through intramolecular hydrogen bond (O2–H2…N1: O2–H2 = 0.082 nm, H2…N1 = 0.1861 nm, O2…N1 = 0.2585 nm, O2–H2…N1 = 147°). Meanwhile, the molecules are linked together by weak intermolecular C–H…O (C6–H6…O1^{iv}: C6–H6 = 0.093 nm, H6…O1 = 0.2393 nm, C6…O1 = 0.3313 nm, C6–H6…O1 = 169.8°; C7–H7…O2^{iv}: C7–H7 = 0.093 nm, H7…O2 = 0.2550 nm, C7…O2 = 0.3443 nm, C7–H7…O2 = 161.1°; symmetry code: (iv) $-x + 1, y + 1/2, -z - 1/2$) hydrogen bonds into a *zigzag* one-dimensional chain running along the *b*-axis (Fig. 7), which are further assembled to form a layer structure (Fig. 7).

Compound **4e** crystallizes in the triclinic space group $P\bar{1}$, and forms crystalline clathrates with DMF in a 2:1 M ratio. In this molecule, there are two crystallographically independent but conformationally almost identical molecules in the asymmetric unit (Fig. 8). Moreover, in each molecule, the carboline moiety appears to be fully planar. The bond geometries show good agreement with each other. However, they differ with respect to torsion angle as well as in the dihedral angles. For example, the dihedral angle between the carboline ring plane and the benzyl phenyl ring plane in B is 81.6°, slightly larger than the value of 75.4° found in A, but less than the corresponding value of 86.1° in **4d**. Likewise, the dihedral angle between the carboline ring and the hydroxyphenyl ring in B is 10.1°, obviously larger than the value of 3.7° found in A.

In the crystal structure, **4e** shows an intramolecular hydrogen bond between the O2 and N4 or O5 and N8 atoms (O2–H2…N4: O2–H2 = 0.082 nm, H2…N4 = 0.1876 nm, O2…N4 = 0.2598 nm, O2–H2…N4 = 146°; O5–H5…N8: O5–H5 = 0.082 nm, H5…N8 = 0.1969 nm, O5…N8 = 0.2687 nm, O5–H5…N8 = 146°), forming a six-membered ring, which is coplanar. Two **4e** and a DMF solvent molecule are linked by intermolecular N–H···O and O–H···O ((N3–H3A···O7: N3–H3A = 0.086 nm, H3A…O7 = 0.2107 nm, N3…O7 = 0.2888 nm, N3–H3…O7 = 151°; O3–H3···O4: O3–H3 = 0.082 nm, H3…O4 = 0.1868 nm, O3…O4 = 0.2685 nm,

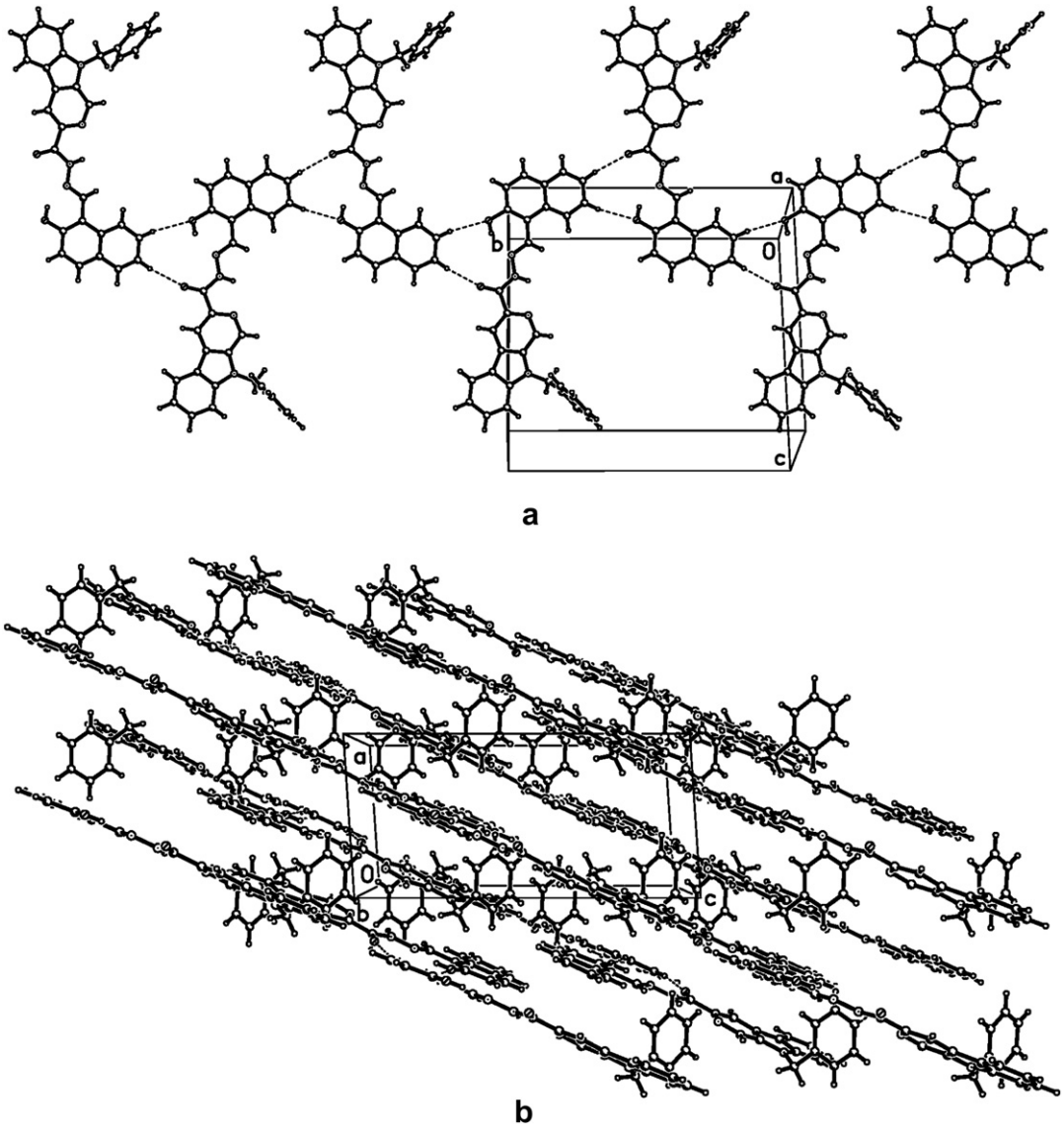

Fig. 7. (a) The one dimensional structure formed *via* hydrogen bonds in **4d**. (b) A packing diagram for **4d**, viewed down the *b* axis.

O3–H3…O4 = 174°) hydrogen bonds into a hydrogen-bonded trimer. Further, the trimers are linked by intermolecular O–H•••O (O6–H6•••O1^{v}: O6–H6 = 0.082 nm, H6…O1 = 0.1871 nm, O6…O1 = 0.2675 nm, O6–H6…O1 = 166°; symmetry code: (v) x, $y + 1$, z) hydrogen bonds into a *zigzag* one-dimensional chain along the *b*-axis (Fig. 9), which are further extended into a three dimensional supramolecular architecture through the weak intermolecular C–H…O hydrogen bonds and π–π stacking interactions (Fig. 9).

The compound **4f** forms crystalline clathrates with DMF in a 1:1 M ratio and crystallizes in the triclinic space group $P\bar{1}$. Both the carboline and hydroxyphenyl rings are rotated out of the plane of the central hydrazone component (Fig. 10), forming dihedral angles of 11.4 and 8.7° with it. Moreover, the planar *β*-carboline ring system makes a dihedral angle of 4.1° with the hydroxyphenyl ring, but forms a dihedral angle of 78.2° with the benzyl phenyl ring. Consequently, the whole compound is not a planar molecule.

As shown for **4a**, **4d** and **4e**, in this compound there is also an intramolecular hydrogen bond between the O2 and N4 atoms (O2–H2•••N4: O2–H2 = 0.082 nm, H2…N4 = 0.1869 nm, O2…N4 = 0.2583 nm, O2–H2…N4 = 145°), forming an S(6) ring motif. On the other hand, the molecules are linked by pair-wise self complementary O3—H3A…O1 (O3–H3A•••O1^{vi}: O3–H3A = 0.082 nm, H3A…O1 = 0.1962 nm, O3…O1 = 0.2710 nm, O3–H3A…O1 = 151°; symmetry code: (vi) $-x$, $-y$, $-z$) hydrogen bonding interactions into a centrosymmetric dimer, with the formation of an $R_2^2(20)$ ring motif as shown in Fig. 11. Two DMF solvent molecules are connected to the dimer on both sides through intermolecular N3–H3…O4 hydrogen bonds (N3–H3…O4: N3–H3 = 0.086 nm, H3…O4 = 0.2053 nm, N3…O4 = 0.2867 nm, N3–H3…O4 = 157°), thus generating the symmetric hydrogen-bonded tetramer (Fig. 11). The tetramers are held together by the weak intermolecular C–H…O hydrogen bonds and π–π stacking interactions to form an extended layer structure (Fig. 11). These structural characteristics of compound **4f** are different from those of in **4e**, though **4f** is an isomer of **4e**.

Notably, four compounds showed three different space groups (orthorhombic space group: $Pca2_1$ for **4a**; monoclinic space group: $P2_1/c$ for **4d**; triclinic space groups: $P\bar{1}$ for **4e** and **4f**). Thus, the introduction of substituents onto carboline-hydrazone unit is considered to change the crystal structure due to the effect of the

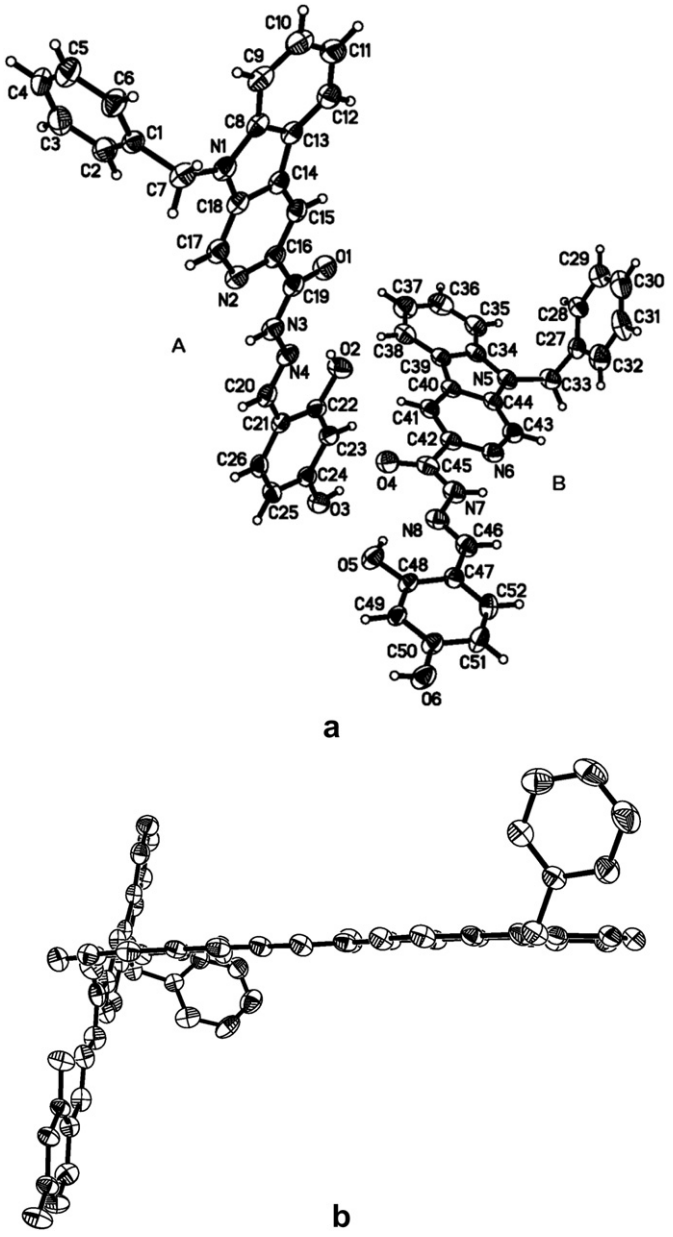

Fig. 8. (a) The molecular structure of **4e**, showing the atom-labeling scheme. Displacement ellipsoids are drawn at the 30% probability level. H atoms are shown as small spheres of arbitrary radius. DMF molecule is omitted for clarity. (b) The side elevation of **4e**. DMF molecule and H atoms are omitted for clarity.

nature and position of the substituents. The formation of ordered structures from these compounds is expected to have a potentially large impact on their optoelectronic properties in the solid state.

3.3. Absorption spectra

UV–vis absorption spectra of these molecules in diluted DMF solutions are given in Fig. 12. As shown in Fig. 12, several absorption peaks could be observed in the linear absorption spectra of **4** in the wavelength range from 250 to 530 nm, while almost no linear absorption was observed beyond 530 nm. Such multi-peak profiles in the linear absorption spectra indicate that these molecules in the excited state suffer structure distortions in the π-conjugated frameworks.

Compounds **4a** and **4d** have similar absorption spectra. Broadly, there are four distinct absorption bands in the range of 250–530 nm. Typically, the first absorption band in the region 400–480 nm reflects an intramolecular charge transfer (ICT) band of the entire conjugated molecule; two intense structured bands, the second and third absorption bands, one covering the range 340–400 nm and the other in the range 300–340 nm, are observed. There is not much difference between the absorption spectra of **4a** and **4d** apart from the nontrivial enhancement of absorption intensity in the long wavelength region for **4a**. This indicates that the N_9-benzylation of the β-carboline nucleus has a slight influence on the absorption spectra and causes only a slight change in the spectra.

Absorption spectral features of **4e** are extremely similar to those of **4b**. The only difference is a slightly red shift of maximum of absorption peak for **4e**. However, in the case of **4f**, the absorption spectrum is characterized by an intense broad absorption from 250 to 380 nm. Within this broad absorption profile there is evidence of three main peaks with λ_{max} values of 265, 296 and 324 nm. Besides, one clear shoulder peak at around 360 nm was also observed in the range of longer wavelength. Nevertheless, these spectral behaviors are different from those of **4e**, though **4f** is an isomer of **4e**. The maximum absorption peak (324 nm) for **4f** is blue-shifted by 18 nm as compared with **4e**. Considering such a hypsochromic shift, one can say that the electronic effect of the 2,3-hydroxyphenyl group is weaker than that of the 2,4-hydroxyphenyl group.

Additionally, it is worth noting that three compounds, **4c**, **4f** and **4g**, have the very similar spectral shape, owing to their very similar structure. Of course, the similarity in the absorption spectra of these compounds suggests that the methylation of **4f** almost does not change the absorption spectrum.

The results above imply that more π-electrons and more extended π-conjugated system may be involved in **4a** and **4d** than those in the other samples. This may be related to the greater electron-donating ability of the end naphthalene unit. As a result, the red-shift of absorption can possibly occur.

3.4. Emission properties

The photoluminescence properties of these molecules in solution are first studied. It can be seen from Fig. 13 that all of compounds, except **4f**, in the present investigation evidence two fluorescence bands, the first one in the range 350–440 nm and the second one centered at around 500 nm. While the strong emission peak 497 nm is observed for **4a** and **4d**, the corresponding emission peak of **4b** and **4e** appears around 500 nm, which showed a slight bathochromic shift. But, for compounds **4c** and **4g**, such a longer wavelength emission is very weak and almost unnoticeable. In the case of **4f**, the fluorescence spectrum is obviously different from those of its analogs (**4b**, **4c**, **4e** and **4g**) due to the absence of emission peak at ~500 nm.

The results above imply that all compounds are fluorescent in solution. Compounds **4a**, **4b** and **4d** present green emission of fluorescence, but the other four compounds have their dominant emission peaks located at 380 nm, which correspond to the ultraviolet (UV) emission.

In most cases, organic fluorophores that fluoresce in solution suffer from fluorescence quenching, showing little or no fluorescence in the solid state. Thus, to gain a deep insight into the solid-state emission behaviors of these derivatives, the solid-state photoluminescence was measured. The solid-state photoluminescence studies were performed at room temperature, using a helium–cadmium laser (325 nm) as the excitation source.

Analysis of the solid-state fluorescence properties of the derivatives reveals an unexpected behavior: under the 325 nm laser

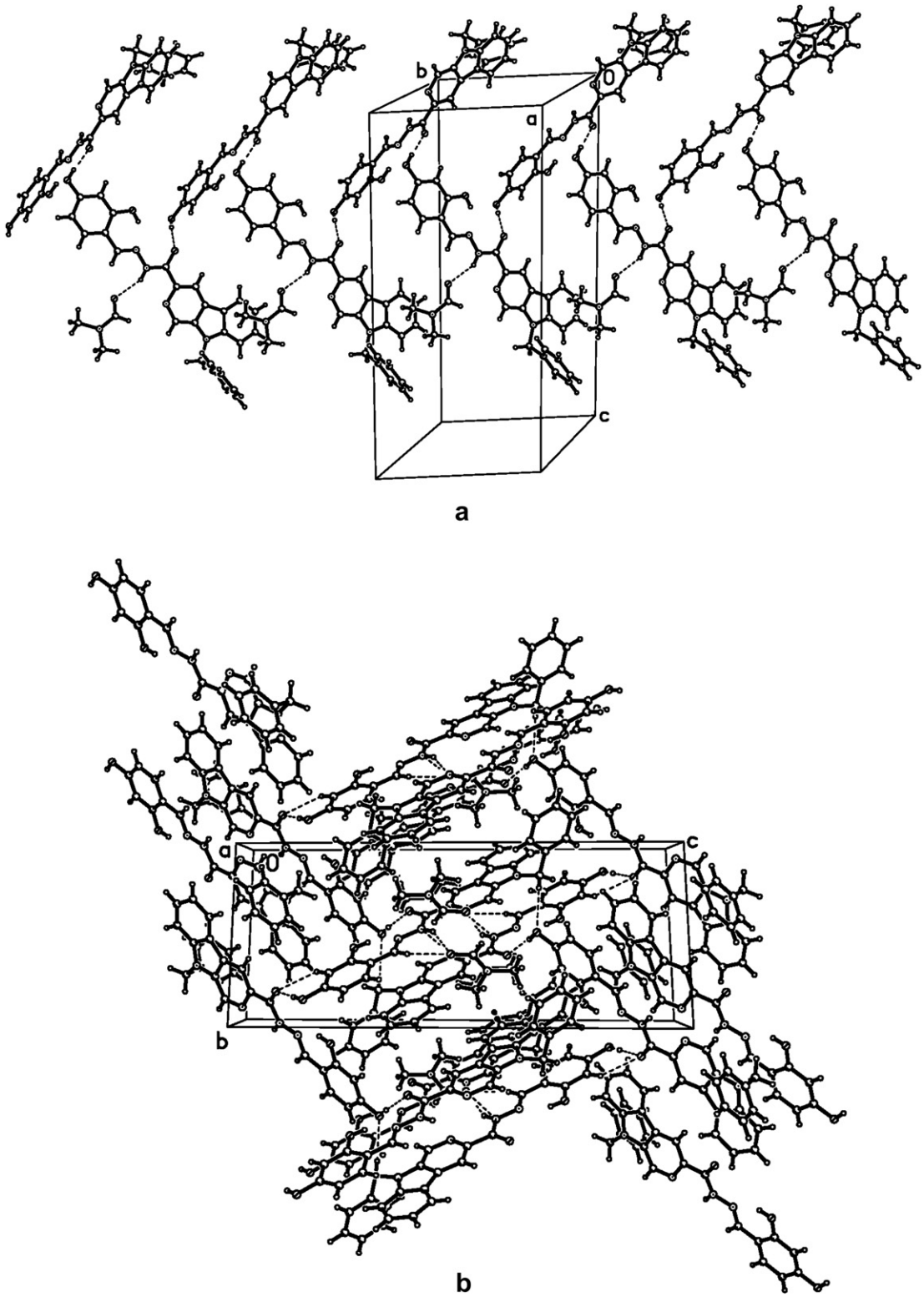

Fig. 9. (a) The one dimensional structure formed *via* hydrogen bonds in **4e**. (b) A packing diagram for **4e**, viewed down the *c* axis.

excitation, all compounds display moderate to intense solid-state fluorescence (Fig. 14). Of seven chromophores only **4f** and **4g** emit yellow light, with the others emitting green light (Fig. 15).

At the same time, in comparison with the data recorded in the dilute solutions, the dyes exhibit very different emissions when in the solid state, as shown in Fig. 14. Obviously, only an emission peak, located in the range of 505–582 nm, could be observed in the solid-state fluorescence spectra of these molecules. Noticeably, in the solid-state case we did not observe the UV band, which was noted for the DMF solution. Moreover, the emission peaks of **4** undergo a red-shift from **4a** (505 nm) to **4e** (520 nm), **4b** (523 nm), **4d** (527 nm), **4c** (540 nm), and to **4f**, **4g** (582 nm).

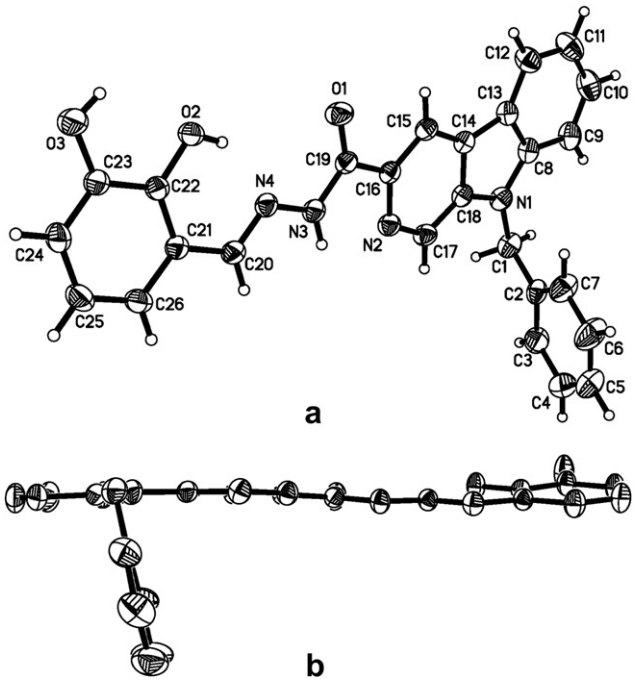

Fig. 10. (a) The molecular structure of **4f**, showing the atom-labeling scheme. Displacement ellipsoids are drawn at the 30% probability level. H atoms are shown as small spheres of arbitrary radius. DMF molecule is omitted for clarity. (b) The side elevation of **4f**. DMF molecule and H atoms are omitted for clarity.

Among these dyes, crystal **4a** shows a very strong green fluorescence emission peak at 505 nm along with a distinct shoulder at about 480 nm, and possesses the highest fluorescence intensity in spite of the shortest peak wavelength of emission relative to the other compounds. Comparison with **4a**, the maximum emission peak of compound **4d** is red-shifted by 22 nm—527 nm, and an extended shoulder on the longer wavelength side of main peak in **4d** is clearly evident. This difference may be attributed to both the N_9-benzylation of the β-carboline nucleus and the packing structure.

Except for a slight blue shift below 3 nm, the observed emission profile of **4e** is almost identical to that of **4b**. Whereas the maximum emission peak of **4f** is significantly red-shifted by 62 nm with respect to that of **4e**. In addition, the maximum emission peak of **4c** is blue-shifted to 540 nm, when compared to **4f** and **4g**, but red-shifted by about 17 nm relative to that of **4b**. Thus, by comparing the emission peaks from **4e** and **4f**, it appears that the hydroxy substitution of β-carbolines at different positions leads to the difference of emission properties.

Besides, a maximum 8-fold increase in fluorescence emission intensity is observed from **4g**, as compared with **4f**, implying that the significant emission enhancement can be attained by the methylation of the 3-OH group of the dihydroxyphenyl ring in **4f**.

Actually, the significant difference of photoluminescence spectra features between in the solution and in the solid state may possibly be attributable to the fact that the photoluminescence spectrum of a luminescent molecule in dilute solution reflects mainly its single molecular characteristics, while the photoluminescence spectrum of the same luminescent molecule in organic crystal form results from the interaction of large numbers of molecules. Consequently, solid dyes exhibit red-shifted emissions, relative to these observed in solution, indicating that interchromophore interactions exist in their packing structures. The presence of the intermolecular interactions has been demonstrated by X-ray diffraction crystal structure analysis in this work. As

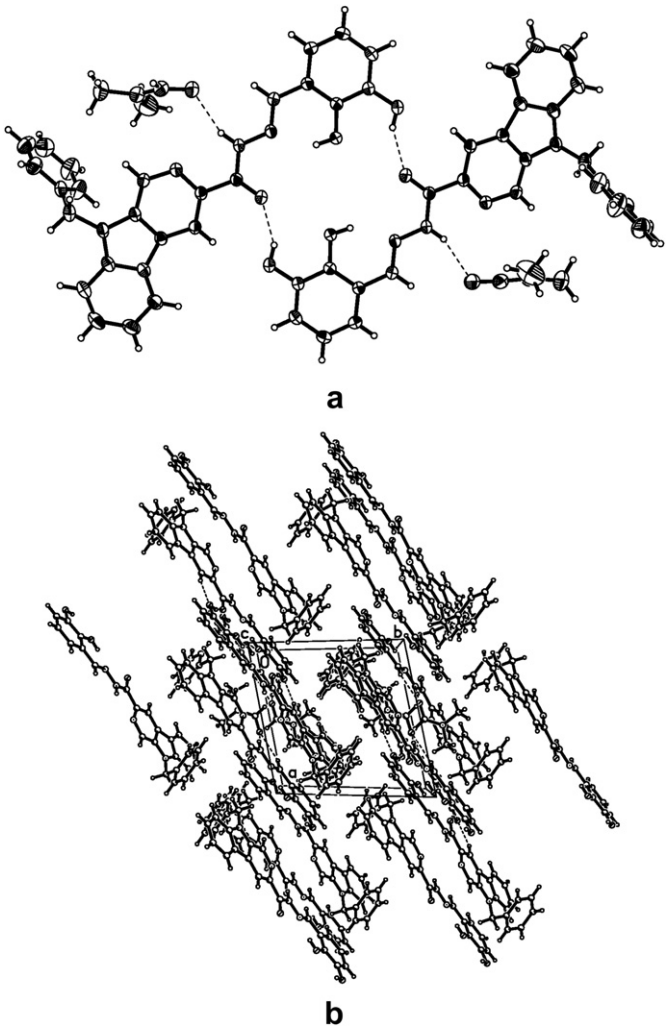

Fig. 11. (a) View of the hydrogen-bonded tetramer in **4f**. (b) A packing diagram for **4f**, viewed down the *c* axis.

mentioned above, the crystal structure analysis results reveal that the main driving forces in the formation of the extended structures are intermolecular hydrogen bonding and π–π stacking interactions.

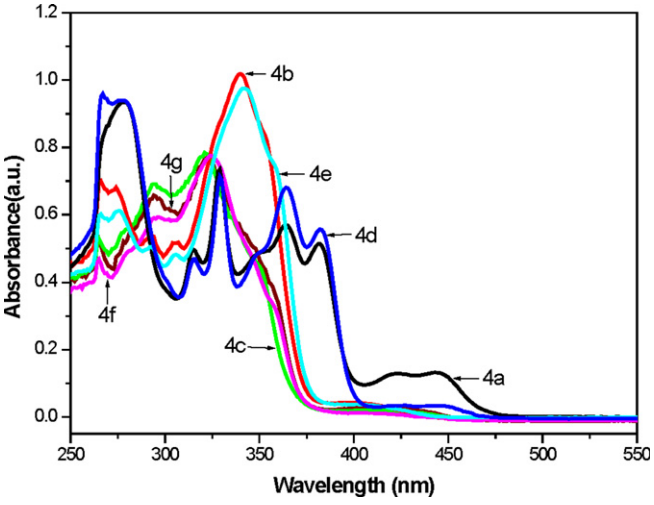

Fig. 12. Absorption spectra of compounds **4** in DMF solution (Concentration: 2.0×10^{-5} M for **4c**, **4d** and **4g**; 2.3×10^{-5} M for the rest).

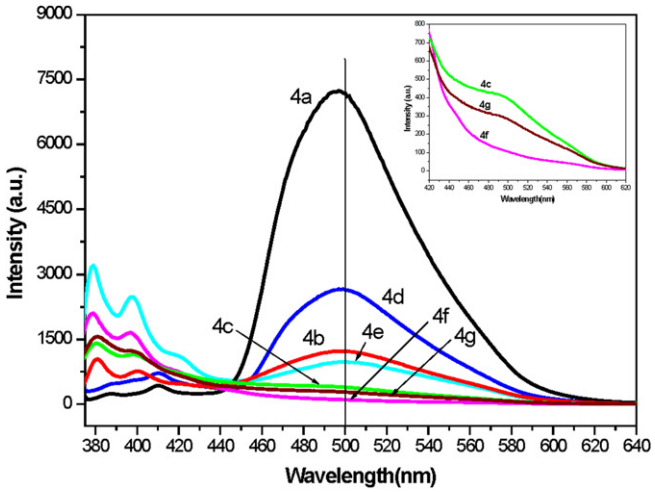

Fig. 13. Photoluminescence spectra of compounds **4** in DMF solution (Concentration: 2.0×10^{-5} M for **4c**, **4d** and **4g** and 2.3×10^{-5} M for the rest; Excitation wavelength: 364 nm for **2a** and **2d**, 342 nm for **2b** and **2e**, 322 nm for **4c**, **4f** and **4g**). The inset depicts the expanded photoluminescence spectra of compounds **4c**, **4f** and **4g**.

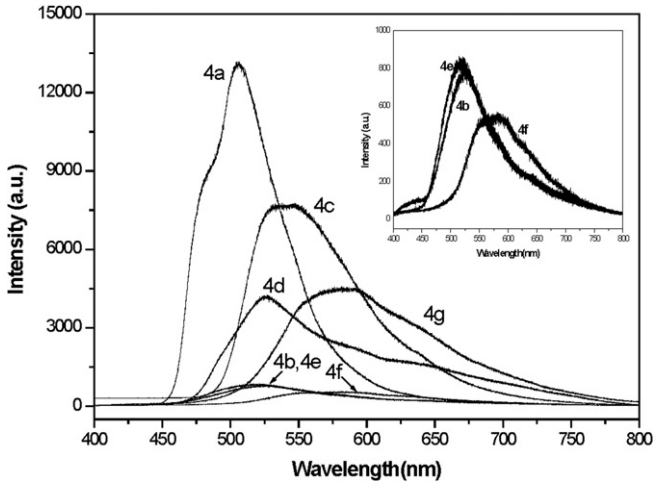

Fig. 14. Photoluminescence spectra of compounds **4** in the solid state. The inset depicts the expanded photoluminescence spectra of compounds **4b**, **4e** and **4f**.

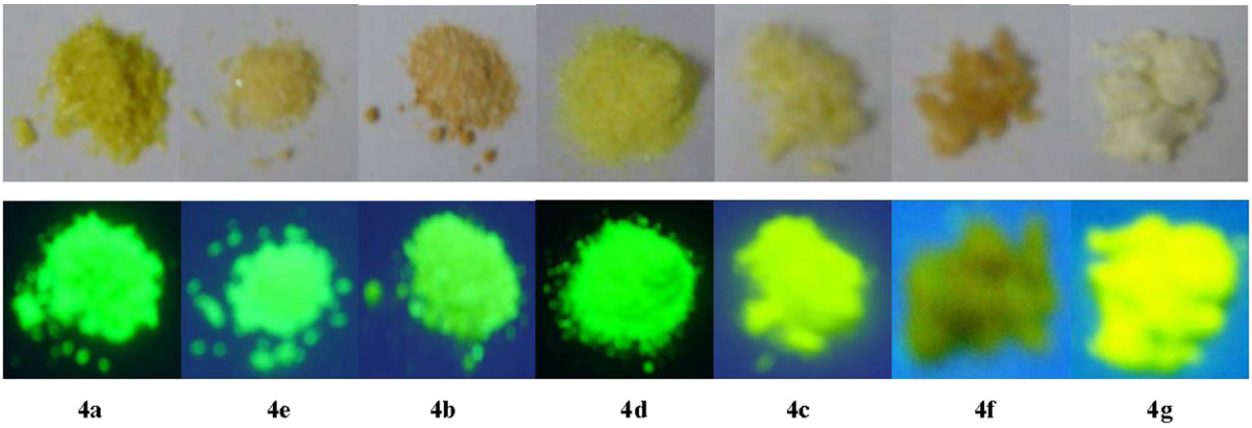

Fig. 15. Photographs of **4** in solid state under room light (top row) and under 365 nm UV light (bottom row).

Considering the above findings, it is strongly suggested that the solid-state luminescent properties are dependent closely on the molecular arrangements and also on the intermolecular interactions of the fluorophores, and the nature and position of the substituents play principle roles in modulation of molecular arrangements in the solid state.

Therefore, it has been concluded that the formation of intermolecular interactions between the fluorophores is responsible for the red-shift of the fluorescence maxima and the remarkable increase in the solid-state fluorescence for **4c** and **4g** from DMF to the solid state. Unfortunately, we could not obtain sufficient sizes of single crystals for **4c** and **4g** to carry out the X-ray structural analysis, however, the relatively strong fluorescence intensity for the crystals of **4c** and **4g** demonstrated that the methylation of the 3-OH group in the dihydroxyphenyl ring can effectively prevent the formation of the dimer through intermolecular hydrogen bonds, thus explaining solid-state emission enhancement from **4c** and **4g**.

4. Conclusions

In summary, in this work, we have reported the synthesis, characterization, structure and photoluminescence properties of a series of organic chromophores based on the β-carboline moiety. X-ray analyses revealed that **4a** crystallize in the orthorhombic space group $Pca2_1$, while **4d** in monoclinic space group $P2_1/c$, and the other two, **4e** and **4f**, were found to be triclinic, with space group $P\bar{1}$. Our findings clearly show that the β-carbolines that are fluorescent in solution display solid-state fluorescence as well. By varying the substituent groups on the carboline unit, the solid-state emission ranging from 505 to 582 nm can be readily obtained. Significantly, compound **4g** shows a strong yellow emission ($\lambda_{max} = 582$ nm) with a maximum 8-fold increase in fluorescence emission intensity as compared with **4f**.

The results showed that the nature and position of the substituents have significant influences on the crystal structure and fluorescence properties. The present study can contribute to the development of efficient fluorescent solid materials.

5. Supplementary material

The crystallographic data (excluding structure factors) of **4a**, **4d**, **4e** and **4f** have been deposited with the Cambridge Crystallographic Center as supplementary publication no. 879,674, 879,675, 879,676 and 879,677, Y, Z AND T. Copy of this information may be obtained free of charge *via* www: http://www.ccdc.cam.ac.uk or from The Director, CCDC, 12 Union Road, Cambridge CB221EZ, UK (fax: +44 1223/336 033; email: deposite@ccdc.cam.ac.uk). Structural factors are available on request from the authors.

Acknowledgments

This work is supported by the Nature Science Foundation of Shandong Province of China (No. ZR2010BM032).

References

[1] Cao R, Peng W, Wang Z, Xu A. β-Carboline alkaloids: biochemical and pharmacological functions. Curr Med Chem 2007;14:479–500.
[2] Chen Z, Cao R, Yu L, Shi B, Sun J, Guo L, et al. Synthesis, cytotoxic activities and DNA binding properties of β-carboline derivatives. Eur J Med Chem 2010;45:4740–5.
[3] Moura DJ, Richter MF, Boeira JM, Henriques JAP, Saffi J. Antioxidant properties of b-carboline alkaloids are related to their antimutagenic and antigenotoxic activities. Mutagenesis 2007;22:293–302.
[4] Chen Z, Cao R, Shi B, Guo L, Sun J, Ma Q, et al. Synthesis and biological evaluation of 1,9-disubstituted β-carbolines as potent DNA intercalating and cytotoxic agents. Eur J Med Chem 2011;46:5127–37.
[5] Ikeda R, Iwaki T, Iida T, Okabayashi T, Nishi E, Kurosawa M, et al. 3-Benzylamino-β-carboline derivatives induce apoptosis through G2/M arrest in human carcinoma cells HeLa S-3. Eur J Med Chem 2011;46:636–46.
[6] Cao R, Peng W, Chen H, Hou X, Guan H, Chen Q, et al. Synthesis and in vitro cytotoxic evaluation of 1,3-bisubstituted and 1,3,9-trisubstituted β-carboline derivatives. Eur J Med Chem 2005;40:249–57.
[7] Wu Q, Cao R, Feng M, Guan X, Ma C, Liu J, et al. Synthesis and in vitro cytotoxic evaluation of novel 3,4,5-trimethoxyphenyl substituted β-carboline derivatives. Eur J Med Chem 2009;44:533–40.
[8] Yang ML, Kuo PC, Hwang TL, Chiou WF, Qian K, Lai CY, et al. Synthesis, in vitro anti-inflammatory and cytotoxic evaluation, and mechanism of action studies of 1-benzoyl-β-carboline and 1-benzoyl-3-carboxy-β-carboline derivatives. Bioorg Med Chem 2011;19:1674–82.
[9] Cao R, Guan X, Shi B, Chen Z, Ren Z, Peng W, et al. Design, synthesis and 3D-QSAR of β-carboline derivatives as potent antitumor agents. Eur J Med Chem 2010;45:2503–15.
[10] Ikeda R, Kurosawa M, Okabayashi T, Takei A, Yoshiwara M, Kumakura T, et al. 3-(3-Phenoxybenzyl)amino-β-carboline: a novel antitumor drug targeting α-tubulin. Bioorg Med Chem Lett 2011;21:4784–7.
[11] Cao R, Chen Q, Hou X, Chen H, Guan H, Ma Y, et al. Synthesis, acute toxicities, and antitumor effects of novel 9-substituted β-carboline derivatives. Bioorg Med Chem 2004;12:4613–23.
[12] Barbosa VA, Formagio ASN, Savariz FC, Foglio MA, Spindola HM, Carvalho JE, et al. Synthesis and antitumor activity of β-carboline 3-(substituted-carbohydrazide) derivatives. Bioorg Med Chem 2011;19:6400–8.
[13] Dorey G, Poissonnet G, Potier MC, Carvalho LP, Venault P, Chapouthier G, et al. Synthesis and benzodiazepine receptor affinities of rigid analogues of 3-carboxy-β-carbolines: demonstration that the benzodiazepine receptor recognizes preferentially the s-cis conformation of the 3-carboxy Group. J Med Chem 1989;32:1799–804.
[14] García-Zubiri IX, Burrows HD, Melo JSS, Monteserín M, Arroyo A, Tapia MJ. A spectroscopic study of the interaction of the fluorescent β-carboline-3-carboxylic acid *N*-methylamide with DNA constituents: nucleobases, nucleosides and nucleotides. J Fluoresc 2008;18:961–72.
[15] Guan H, Liu X, Peng W, Cao R, Ma Y, Chen H, et al. β-Carboline derivatives: novel photosensitizers that intercalate into DNA to cause direct DNA damage in photodynamic therapy. Biochem Biophys Res Commun 2006;342:894–901.
[16] Molero ML, Hazen MJ, Gorrono AIP, Stockert JC. Simple β-carboline alkaloids as nucleic acids fluorochromes. Acta Histochem 1995;97:165–73.
[17] Ghiggino KP, Skilton PF, Thistlethwaite PJ. β-Carboline as a fluorescence standard. J Photochem 1985;31:113–21.
[18] Pardo A, Reyman D, Poyato JML, Medina F. Some β-carboline derivatives as fluorescence standards. J Lumin 1992;51:269–74.
[19] Reyman D, Pardo A, Poyato JML. Phototautomerism of β-Carboline. J Phys Chem 1994;98:10408–11.
[20] Coronilla AS, Carmona C, Munoz MA, Balon M. Ground state isomerism and dual emission of the β-carboline anhydrobase (N_2-methyl-9H-pyrido [3,4-*b*] indole) in aprotic solvents. Chem Phys 2006;327:70–6.
[21] Reyman D, Tapia MJ, Carcedo C, Vinas MH. Photophysical properties of methyl β-carboline-3-carboxylate mediated by hydrogen-bonded complexes – a comparative study in different solvents. Biophys Chem 2003;104:683–96.
[22] Gonzalez MM, Arnbjerg J, Denofrio MP, Erra-Balsells R, Ogilby PR, Cabrerizo FM. One- and two-photon excitation of β-carbolines in aqueous solution: pH-dependent spectroscopy, photochemistry, and photophysics. J Phys Chem A 2009;113:6648–56.
[23] Reyman D, Vinas MH, Tardajos G, Mazario E. The impact of dihydrogen phosphate anions on the excited-state proton transfer of harmane. Effect of β-cyclodextrin on these photoreactions. J Phys Chem A 2012;116:207–14.
[24] Coronilla AS, Carmona C, Muñoz MA, Balón M. Ground and singlet excited state pyridinic protonation of N_9-methylbetacarboline in water-N, N-dimethylformamide mixtures. J Fluoresc ;19:1025–35.
[25] Lippke KP, Schunack WG, Wenning W, Muller WE. β-Carbolines as benzodiazepine receptor ligands. 1. Synthesis and benzodiazepine receptor interaction of esters of β-carboline-3-carboxyliAc cid. J Med Chem 1983;26:499–503.
[26] Cain M, Weber RW, Guzman F, Cook JM, Barker SA, Rice KC, et al. β-Carbolines: synthesis and neurochemical and pharmacological actions on brain benzodiazepine receptors. J Med Chem 1982;25:1081–91.
[27] Dodd RH, Ouannes C, Carvalho LP, Valin A, Venault P, Chapouthier G, et al. 3-Amino-β-carboline derivatives and the benzodiazepine receptor. synthesis of a selective antagonist of the sedative action of diazepam. J Med Chem 1985;28:824–8.
[28] Cao R, Chen H, Peng W, Ma Y, Hou X, Guan H, et al. Design, synthesis and *in vitro* and *in vivo* antitumor activities of novel β-carboline derivatives. Eur J Med Chem 2005;40:991–1001.
[29] Muir AKS, Codding PW. Structure–activity studies of β-carbolines. 3. Crystal and molecular structures of methyl β-carboline-3-carboxylate. Can J Chem 1985;63:2752–6.